Title	An optimized Gaussian beam for multicell indoor optical wireless communications
Author(s)	Wu, Dehao; Ghassemlooy, Zabih; Zhong, Wende; Chen, Chen
Citation	Wu, D., Ghassemlooy, Z., Zhong, W., & Chen, C. (2015). An optimized Gaussian beam for multicell indoor optical wireless communications. Microwave and optical technology letters, 57(5), 1049-1052.
Date	2015
URL	http://hdl.handle.net/10220/25751
Rights	© 2015 Wiley Periodicals Inc. This is the author created version of a work that has been peer reviewed and accepted for publication by Microwave and Optical Technology Letters, Wiley Periodicals Inc. It incorporates referee's comments but changes resulting from the publishing process, such as copyediting, structural formatting, may not be reflected in this document. The published version is available at: [http://dx.doi.org/10.1002/mop.29015].

An Optimized Gaussian Beam for Multi-Cell Indoor Optical Wireless Communications

Dehao Wu, Zabih Ghassemlooy, Wen-de Zhong, and Chen chen

***Abstract*—The characteristics of a multipath indoor optical wireless channel can be estimated by two parameters: optical channel path loss (OCPL) and the root mean square (RMS) delay spread. In this letter, an optimized Gaussian beam (OGB) is proposed for a cellular indoor optical wireless communications (CI-OWC) system. The expression for OGB with an optimized beam waist radius (OBWR) for OGB is derived. OCPL and the RMS delay spread (D_{rms}) for four different configurations are simulated and analyzed. Results show that, for a CI-OWC system, a minimum OCPL can be achieved by using the OGB and the maximum transmission data rate (MTDR) can be significantly extended by increasing the number of cells.**

***Index Terms*—Indoor optical wireless communications, optimized Gaussian beam, RMS delay spread and transmission data rate.**

I. Introduction

RECENT CI-OWC systems using laser diodes (LDs) hold the promise to achieve extreme high transmission bandwidth. Compared with traditional radio frequency (RF) technologies, OWC systems offer several advantages including a large unlicensed bandwidth (orders of magnitude wider than RF), immunity to electromagnetic interference, and a secure link as rays cannot penetrate walls or opaque objects. With an increasing requirement of high data rates transmission for future indoor communication systems, CI-OWC technology is seen as an attractive solution to unlock the bandwidth congestion in local area and access networks [1].

Recent research on CI-OWC systems has mainly focused on achieving improved optical power distributions as well as reduced multipath distortion. A genetic algorithm controlled multi-spot indoor OWC system is proposed in [2] to achieve a uniform power distribution but not at the cost of bandwidth, which is quite useful for designing an optimum receiver. However, the transmission bandwidth is still limited to ~ 20 MHz. In [3], a novel transmitter arrangement is outlined that significantly reduces the fluctuation of power distribution and ensures that same quality of service for all users regardless of their locations. A multi-spot diffuse configuration with an angle diversity detection is proposed for an indoor OWC system in [4], which improves the signal to noise ratio (SNR) by more than ~11 dB. However, such systems with composite receivers (7 branches) are very complicated and costly. Additionally, in [2-4], the divergence angle (DA) of transmitter hasn't been investigated, which could significantly affect the transmission bandwidth. Spotlighting with a small DA for a CI-OWC link is proposed in [5] with higher MTDR. This study shows that indoor OWC systems with a small DA would offer much reduced multipath induced distortion and a high MTDR. In our previously study, we proposed a single-cell CI-OWC system using a diffuse Gaussian beam (DGB)that provides a higher MTDR compared to Lambertian beam (LB) [6]. However, the optimum value of the DA for different configurations hasn't been investigated. To achieve an optimum consumed power efficiency and a higher MTDR, a multi-cell CI-OWC system using DGB with an optimized DA is proposed in this letter. Firstly, we derive an expression for OGB with an OBWR. Then, the minimum OCPL and D_{rms} are characterized for four different cell configurations. Finally, the corresponding MTDRs of four different scenarios are compared and discussed.

The rest of the paper is organized as follow. In section II, the system configuration, OGB and multipath characteristics are described. In section III, the simulation results are presented and discussed. In section IV, conclusion is given.

II. Channel Characteristics

A. System configuration

The proposed CI-OWC system employing OGB is shown in Fig.1. OGB is produced by a single mode LD and a light shape diffuser (LSD). The room model has a dimension of 5 × 5 × 3 m^3 (width, length and height) and the ceiling plane is split into n (where $n = i \times j$) identical cells. Each cell identified as C_{ij} has a cell radius R. A LD with a LSD is located at the centre of each cell pointing downward to the receiver plane. An optical receiver with a dedicated field of view (FOV) is mounted at a mobile terminal pointing upward to the ceiling to ensure a seamless connectivity.

B. Optimized Gaussian beam

The irradiance distribution of the fundamental Gaussian TEM_{00} laser beam at distance z is given by [7]:

$$I(r,z) = I_0 \exp(-\frac{2r^2}{\omega^2(z)}) = \frac{2P_t}{\pi\omega^2(z)} \exp(-\frac{2r^2}{\omega^2(z)}), \quad (1)$$

where I_0 is the centre axial intensity, P_t is the total transmitted optical power of the beam, r is the horizontal distance between LD and the point (x, y) at the terminal plane, Fig. 1,

Dehao Wu, Wen-de Zhong and Chen chen are with School of Electrical and Electronic Engineering, Nanyang Technological University, 50 Nanyang Avenue, Singapore 639798. (e-mail:dehao.wu@ntu.edu.sg).

Zabih Ghassemlooy is with Optical Communications Research Group, Faculty of Engineering and Environment, Northumbria University, Newcastle upon Tyne, NE1 8ST, U.K.

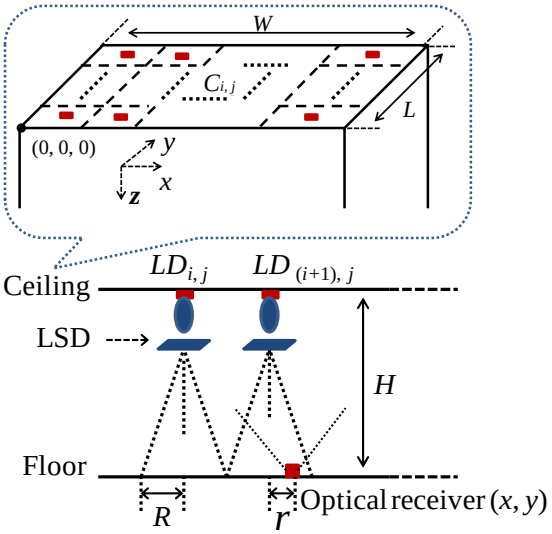

Fig.1. A CI-OWC system employing an OGB.

and function $w(z)$ describes the evolution of the optical beam along the propagation direction z given by [7]:

$$\omega(z) = \omega_0 \left[1 + \left(\frac{\lambda z}{\pi \omega_0^2}\right)^2\right]^{0.5}, \quad (2)$$

where λ is the wavelength of light, ω_0 is the spot size radius (i.e. the radius where the field amplitude value drops to e^{-1} of the centre value) at the propagation distance $z = 0$. For the proposed CI-OWC link with a wider covering area, the laser beam is passed through an optical LSD. In our previous study, an extended irradiance distribution of a circular DGB is given by [6]:

$$P_{\text{r\_CGB}}(r, z) = \frac{\ln 2 P_t A_R}{\pi \omega_{\text{FWHM}}^2(z)} \exp\left(-\frac{\ln(2)\, r^2}{\omega_{\text{FWHM}}^2(z)}\right). \quad (3)$$

where, A_R is the photodetector surface area. $\omega_{\text{FWHM}}(z)$ is the diffused beam waist radius based on the full width at a half maximum (FWHM) divergence angle given by [6]:

$$\omega_{\text{FWHM}}(z) = H \tan(\tfrac{1}{2}\phi_{\text{LSD}}), \quad (4)$$

where, ϕ_{LSD} is the FWHM angle of LSD, H is the height of the room and $\omega_{1/e}(z)$ is the diffused beam waist radius based on full width at the 1/e maximum angle, which is given by [6]:

$$\omega_{1/e}(z) = \sqrt{\frac{2}{\ln 2}}\, \omega_{\text{FWHM}}(z), \quad (5)$$

In a CI-OWC system, see Fig.1, the received optical power P_r at the floor level is composed of power from LOS and reflected paths. To reduce OCPL, the DA of the diffused beam should be as small as possible to avoid optical power being absorbed by the reflectors. However, the DA of diffused beam also should be as large as possible to offer a large footprint covering the entire room. Therefore, to achieve an optimum OCPL for CI-OWC system, an optimum DA of the diffused beam needs to be determined. P_r from the LOS path within each cell can be calculated using (3). For each cell C_{ij}, see Fig. 1, P_r is maximum and minimum at $r = 0$ and $r = R$, respectively. Using (3) and (5) the maximum and minimum optical powers are given by:

$$P_{\text{r-max}}(0, z) = \frac{2 P_t A_R}{\pi \omega_{1/e}^2(z)}, \quad (6)$$

$$P_{\text{r-min}}(R, z) = \frac{2 P_t A_R}{\pi \omega_{1/e}^2(z)} \exp\left(-\frac{2R^2}{\omega_{1/e}^2(z)}\right). \quad (7)$$

The partial derivative of (7) in terms of $\omega_{1/e}(z)$ at a propagation distance z is given by:

$$\frac{\partial P_{\min}(R,z)}{\partial\, \omega_{1/e}(z)} = \frac{2PA_R}{\pi \omega_{1/e}^3(z)} \exp\left(-\frac{2R^2}{\omega_{1/e}^2(z)}\right)\left[\frac{4R^2}{\omega_{1/e}^2(z)} - 2\right], \quad (8)$$

Since $\frac{2PA_R}{\pi \omega_{1/e}^3(z)} > 0$, $\exp\left(-\frac{2R^2}{\omega_{1/e}^2(z)}\right) > 0$ and $\omega_{1/e}(z) \in (0, \infty)$, we have:

$$\frac{\partial P_{\min}(R,z)}{\partial\, \omega_{1/e}(z)} \begin{cases} > 0,\ \omega_{1/e}(z) \in (0, \sqrt{2}R), \\ = 0,\ \omega_{1/e}(z) = \sqrt{2}R, \\ < 0,\ \omega_{1/e}(z) \in (\sqrt{2}R, \infty). \end{cases} \quad (9)$$

Therefore, $\forall\ \omega_{1/e}(z) \in (0, \infty)$, $P_{\text{r-min}}(R, z)$ has only one maximum value, which is given by the condition of $\omega_{1/e}(z) = \sqrt{2}R$. We define this maximum value as the optimum received optical power given by (7):

$$P_{\text{r-min\_opt}}(R, z) = \frac{2 P_t A_R e^{-1}}{\pi R^2}, \quad (10)$$

The corresponding optimum beam waist radius is given by:

$$\omega_{\text{opt}}(z) = \sqrt{2}R, \quad (11)$$

In this letter, a circular DGB with the optimized FWHM divergence angle is defined as OGB for the proposed CI-OWC system. This optimized angle is given by using (4) and (5) as:

$$\phi_{\text{LSD\_opt}}(z) = 2 \tan^{-1}\left(\frac{R\sqrt{\ln 2}}{H}\right). \quad (12)$$

An elliptical beam is proposed in [8] to improve the transmission bandwidth for an indoor OWC system in a rectangular room. Similarly, an extended irradiance distribution of an elliptical DGB can be derived from (3), which is given by:

$$P_{\text{r\_EGB}}(x, y, z) = \frac{\ln 2 P_t A_R}{\pi\, \omega_{\text{FWHM\_x}(z)}\, \omega_{\text{FWHM\_y}(z)}} \exp\left(-\frac{\ln(2)\, x^2}{\omega_{\text{FWHM\_x}}^2(z)} - \frac{\ln(2)\, y^2}{\omega_{\text{FWHM\_y}}^2(z)}\right). \quad (13)$$

where, $\omega_{\text{FWHM\_x}}(z)$ and $\omega_{\text{FWHM\_y}}(z)$ are the diffused beam waist radii at x axis and y axes, respectively.

C. *Multipath characteristics*

In the proposed CI-OWC system, the multipath-induced dispersion will limit MTDR. The geometry of the link with a multi-cell configuration is shown in Fig. 2. The optical power distribution and the multipath dispersion at the receiver plane can be characterized by the channel impulse response $h(t)$. For a LOS channel, the irradiance distribution of a source using a DGB radiation pattern has a uni-axial symmetry as shown in (3). The LOS impulse response for a particular source $LD_{i,j}$ and a photodetector (PD) (x, y, z), is given by [9]:

$$h^0\left(t; LD_{i,j}, \text{PD}\right) = \frac{P_r(r,z)}{P_t} A_R \cos\theta_0\, \text{rect}\left(\frac{\theta_0}{FOV_d}\right)\delta\left(t - \frac{d_0}{c}\right), \quad (14)$$

where θ_0 is the LOS incidence angle, FOV_d is the field of view of PD, d_0 is the LOS distance between $LD_{i,j}$ and PD, t is the delay time of propagation and c is the speed of light (see Fig. 2). The rectangular function $\text{rect}(x)$ is given by:

$$\text{rect}(x) = \begin{cases} 1 & \text{for } |x| \le 1, \\ 0 & \text{for } |x| > 1. \end{cases} \quad (15)$$

In [10], Lomba proposed a Phong model to approximate the reflection pattern of an indoor OWC diffuse channel.

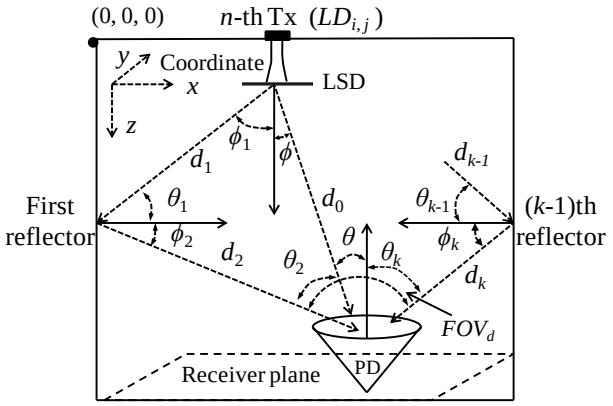

Fig.2. Geometry of source, detector and reflector

Compared with Lambertian model, Phong model is more precise for specular surfaces. However, it is more complex and is almost the same as Lambertian model when modeling rough surfaces. In this letter, assuming that all reflectors (i.e. plaster and acoustic-tiled walls, unvarnished wood) are approximately Lambertian [9], the channel impulse response with multiple optical sources and multiple reflections is given by [11]:

$$h\left(t; LD_{i,j}, \mathrm{PD}\right) = \sum_{i=1,j=1}^{N_{\mathrm{source}}} \sum_{k=0}^{\infty} h_n^k\left(t; LD_{i,j}, \mathrm{PD}\right). \quad (16)$$

$h\left(t; LD_{i,j}, \mathrm{PD}\right)$ for exactly k-bounce with the extension for DGB pattern is given by [11]:

$$h^k\left(t; LD_{i,j}, \mathrm{PD}\right) = \int_{\Psi} \left[\xi_0 \xi_1 \ldots \xi_k \rho^k \,\mathrm{rect}\left(\frac{\theta_k}{FOV_d}\right) \times \delta\left(t - \left(\frac{\sum_{k=0}^{\infty} d_k}{c}\right)\right)\right] dA_{ref}\ ,\ k \geq 1 \quad (17)$$

where,

$\xi_0 = \frac{P_r(r,z)}{P_t} dA_{ref} \cos\theta_1$, $\xi_1 = \frac{dA_{ref} \cos\emptyset_2 \cos\theta_2}{\pi d_2^2}$, ... ,

$\xi_k = \frac{A_R \cos\emptyset_{k+1} \cos\theta_{k+1}}{\pi d_{k+1}^2}$.

where dA_{ref} is the small area of the reflecting element, ϕ_k and θ_k are the angles of irradiance and incidence, respectively, and d_k is the distance from k-bounce to the detector (see Fig. 2). The integration in (15) is performed with respect to the surface Ψ of all reflectors,

The RMS delay spread can be calculated using $h(t)$ given by [9]:

$$D_{\mathrm{rms}} = \left[\frac{\int (t-\mu)^2 h^2(t) dt}{\int h^2(t) dt}\right]^{\frac{1}{2}}, \quad (18)$$

The mean delay μ is given by:

$$\mu = \frac{\int t\, h^2(t) dt}{\int h^2(t) dt} \quad (19)$$

III. Results and Discussion

The channel characteristics including OCPL and D_{rms} for CI-OWC system are simulated and analysed. With the computational time for calculating the impulse response is proportional to k^2 [12], the bounces of impulse response is limited as $k = 2$. In addition, the resulting impulse response in (14) requires smoothing by subdividing the time into bins of width Δt and summing the total power in each bin [13]. In this investigation, a single bin width of 0.1 ns is used. The rest of the specifications and key parameters are given in Table I. Four different cell configurations are considered.

A. Optical channel path loss

In the proposed multi-cell CI-OWC system, each cell has the same performance of OCPL. $P_{\text{r-min}}$ at the receiver plane within one cell can be calculated using (7). Normalizing P_t to 1 W for the entire room, Fig. 3 illustrates $P_{\text{r-min}}$ against a range of ϕ_{LSD} of transmitter for four different cell configurations. It is shown that to achieve a minimum OCPL, $\phi_{\mathrm{LSD\_opt}}$ of the optimized DGB are 22º, 28º, 36º and 52º for 25, 16, 9 and 4 cells configurations, respectively. Results in Fig. 3 (plotted using (4), (5) and (7)) agree well with the calculation values using (12). Besides, using (11) the corresponding OBWRs of OGBs for these scenarios are 2.5 m, 1.66 m, 1.25 m and 1 m, respectively. $P_{\text{r-min}}$ of ~ -34 dBm is the same for four cases. It is also noticed that $\phi_{\mathrm{LSD\_opt}}$ of DGB is critical for a 4-cell case as there is a sharp fall in $P_{\mathrm{r-min\_opt}}$ when ϕ_{LSD} increases or decreases from the optimum value.

B. RMS delay spread

In order to determine the channel transmission bandwidth within the entire room, the D_{rms} is investigated in this section. Using the specifications given in Table I, the RMS delay spreads for the four different cell configurations with $\phi_{\mathrm{LSD\_opt}}$ are depicted in Figs. 4(a) to (d) using (12) and (18). It is shown that with increasing the number of cells as well as reducing the corresponding cell size, a significant reduction of

TABLE I
SPECIFICATION FOR THE CI-OWC SYSTEM

Transmitter beam radius (w_0)	0.1 mm
Total launched power within the room	1 W
Half angle FOV of the receiver	60 (deg)
Surface area of photodiode	16 mm^2
Reflection coefficient (wall, ceiling, floor)	(0.8, 0.8, 0.3)

Cell configurations	Cell size (R) (meter)	Launched power per cell (Watt)
4-cell	1.77	$1/4$
9-cell	1.18	$1/9$
16-cell	0.88	$1/16$
25-cell	0.71	$1/25$

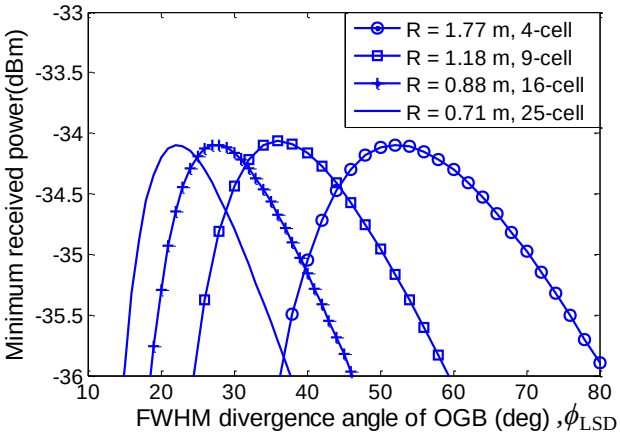

Fig.3. Minimum received optical power as total power normalized to 1 W.

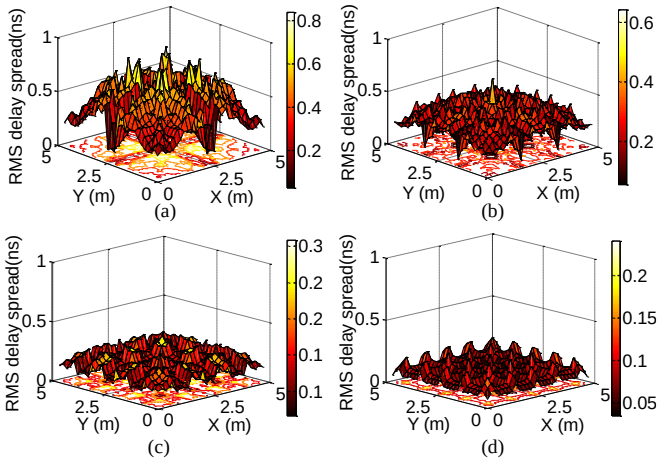

Fig.4. RMS delay spread for multi-cell CI-OWC system a) 4-cell, b) 9-cell, c) 16-cell and d) 25-cell.

TABLE II
SIMULATION RESULTS FOR 4-CELL LINKS WITHIN RECTANGULAR ROOM

Room (length, width, height)	$6 \times 4 \times 3$ m^3	
Beam pattern	$\overline{D_{\text{rms}}}$ (Mean) [ns]	$D_{\text{rms\_Max}}$ (Maximum) [ns]
Elliptical GB (LD) $65^o \times 31^o$ (semi-angle)	1.29	1.88
LB (LEDs) 60^o (semi-angle)	1.88	2.62

D_{rms} is observed due to the decreased divergence angles. The maximum RMS delay spreads are ~0.8 ns, ~0.6 ns, ~0.3 ns and ~0.25 ns for 4, 9, 16 and 25 cells configurations, respectively. As the maximum D_{rms} corresponds to the largest multipath distortion, which limits the transmission bandwidth of the room, the maximum transmission data rate through the CI-OWC channel can be calculated following [14], which is given by:

$$R_b \leq \frac{1}{10 D_{\text{rms\_Max}}}. \quad (20)$$

where $D_{\text{rms\_Max}}$ is the maximum D_{rms} within a room. Therefore, MTDRs for the proposed 4, 9, 16 and 25 cells CI-OWC systems using OGB are ~125 Mbit/s, ~167 Mbit/s, ~333 Mbit/s and ~400 Mbit/s, respectively. We observe significant improvements in MTDR when the number of cells increases.

In addition, an elliptical GB is proposed for a rectangular room in order to reduce the multipath distortion. Employing the optimal turned divergence angles of an elliptical beam in [8], a 4-cell OWC link based on a elliptical GB or a LB is characterized in Table II. The result show that the mean RMS delay spread $\overline{D_{\text{rms}}}$ of the elliptical GB case is ~1.29 ns, which is less than 1.88 ns of the standard LB. $D_{rms\text{-}Max}$ are ~1.88 and ~2.62 for elliptical GB and LB, respectively. MTDR for a 4-cell link within a rectangular room can be calculated from (20), which shows that the turned elliptical GB link has larger MTDR compared to a standard LB.

IV. CONCLUSION

A multi-cell configuration with an OGB has been proposed for a CI-OWC system in order to improve MTDR as well as to achieve a minimum OCPL. An expression for OGB is derived and proposed, and the corresponding OCPL and D_{rms} are simulated and discussed. Compared to the channel characteristics of four different cell configurations, we have shown that MTDR can be improved for CI-OWC systems by increasing the number of cells as well as reducing the cell size. Furthermore, the improvement does not result in additional transmitted optical power. However, more transmitters would be needed as the number of cells increases.

REFERENCES

[1] Ke, W., Nirmalathas, A., Lim, C. and Skafidas, E. 4×12.5 Gb/s WDM optical wireless communication system for indoor applications. *Lightwave Technology, Journal of*, 29, 13 2011), 1988-1996.
[2] Higgins, M. D., Green, R. J. and Leeson, M. S. A Genetic Algorithm Method for Optical Wireless Channel Control. *Lightwave Technology, Journal of*, 27, 6 2009), 760-772.
[3] Zixiong, W., Changyuan, Y., Wen-De, Z., Jian, C. and Wei, C. Performance of a novel LED lamp arrangement to reduce SNR fluctuation for multi-user visible light communication systems. *Opt. Express*, 20, 4 2012).
[4] Jivkova, S. and Kavehard, M. Multispot diffusing configuration for wireless infrared access. *IEEE Trans. Commun.*,, 48, 6 2000), 970-978.
[5] Borogovac, T., Rahaim, M. and Carruthers, J. B. *Spotlighting for visible light communications and illumination*. City, 2010.
[6] Wu, D., Ghassemlooy, Z., Minh, H. L., Rajbhandari, S. and Boucouvalas, A. C. Improvement of the Transmission Bandwidth for Indoor Optical Wireless Communication Systems Using a Diffused Gaussian Beam. *Communications Letters, IEEE*, 16, 8 2012), 1316-1319.
[7] Goldsmith, P. *Gaussian Beam Quasioptical Propogation and Applications*. Wiley-IEEE Press, 1998.
[8] Wu, D., Ghassemlooy, Z., Rajbhandari, S., Le Minh, H. and Boucouvalas, A. C. Improvement of Transmission Bandwidth for Indoor Optical Wireless Communication Systems Using an Elliptical Lambertian Beam. *Photonics Technology Letters, IEEE*, 25, 2 2013), 107-110.
[9] Carruthers, J. B. and Carroll, S. M. Statistical impulse response models for indoor optical wireless channels. *International Journal of Communication Systems*, 18, 3 2005), 267-284.
[10] Lomba, C. R., Valadas, R. T. and Duarte, A. M. d. O. Experimental characterisation and modelling of the reflection of infrared signals on indoor surfaces. *Optoelectronics, IEE Proceedings* -, 145, 3 1998), 191-197.
[11] Kwonhyung, L., Hyuncheol, P. and Barry, J. R. Indoor channel characteristics for visible light communications. *IEEE Communications Letters*, 15, 2 2011), 217-219.
[12] Carruthers, J. B. and Kannan, P. Iterative site-based modeling for wireless infrared channels. *IEEE Transactions on Antennas and Propagation*, 50, 5 2002), 759-765.
[13] Barry, J. R., Kahn, J. M., Krause, W. J., Lee, E. A. and Messerschmitt, D. G. Simulation of multipath impulse response for indoor wireless optical channels. *IEEE Journal on Selected Areas in Communications*, 11, 3 1993), 367 - 379.
[14] Rappaport, T. S. *Wireless Communications*. Prentice-Hall, 2002.